Journal of Thermal Engineering
Yildiz Technical University Press, Istanbul, Turkey
Vol. 1, Issue No. 1, pp. 1-9, January, 2015.

http://eds.yildiz.edu.tr/journal-of-thermal-engineering/Articles
Manuscript Received May 12, 2014; Accepted June 10, 2014

This paper was recommended for publication in revised form by Editor-in-Chief Ahmet Selim Dalkilic

INVERTED FINS FOR COOLING OF A NON-UNIFORMLY HEATED DOMAIN

***Erdal Çetkin**
Izmir Institute of Technology,
Department of Mechanical
Engineering
Urla, Izmir, Turkey

Keywords: Constructal; Inverted fins; Vascular; Non-uniform heating; Conductive cooling; Tree-shaped
** Corresponding author: E. Çetkin, Phone: +90(232)750-6713, Fax: +90(232)750-6701*
E-mail address: erdalcetkin@iyte.edu.tr

ABSTRACT

This paper shows that the peak temperature of a non-uniformly heated region can be decreased by embedding high-conductivity tree-shaped inserts which is in contact with a heat sink from its stem. The volume fraction of the high-conductivity material is fixed, and so is the volume of the solid region. The length scale of the solid domain is L. Inside there is a cube-shaped region with length scale of 0.1L and heat production 100 times greater than the rest of the domain. The location of this hot spot was varied to uncover how its location affects the peak temperature and the design of inverted fins, i.e. high-conductivity tree-shaped inserts. The volume fraction of the high-conductivity tree was varied for number of bifurcation levels of 0, 1 and 2. This showed that increasing the number of the bifurcation levels decreases the peak temperature when the volume fraction decreases. The optimal diameter ratios and optimal bifurcation angles at the each junction level are also documented. Y-shaped trees promise smaller peak temperatures than T-shaped trees. The location of the vascular tree in the z direction also affects the peak temperature when the heat generation is non-uniform. In addition, the peak temperature is minimum when z = 0.65L even though the hot spot is located on z = 0.75L.

INTRODUCTION

Advanced technologies require compactness such as smaller computers, engines, turbines and so on with significant heat generation rates. For example, Fig. 1 shows how the heat generation in processor chips increases relative to years [1]. Nowadays, power density of an electronic chip is equivalent to the heat generation rate of nuclear reactors. Because compactness is one of the constraints, the volume of the coolant is limited. In addition, fans, pumps and cooling surfaces require additional volume. The spacing in between two cooling channels may not be small enough to cool the system under an allowable temperature level as compactness increases. Therefore, compactness of heat generating systems are limited with the cooling requirements. The compact designs with high power are the direction of the evolution of technology [2]. Therefore, it is essential to design compact cooling systems with great cooling capacities.

Convection promises great cooling performance. Therefore, the literature of the cooling technologies has evolved from natural convection to forced convection and from single phase fluids to phase change and nanofluids [3-11]. However, in a convective cooling system fluid always interact with solid domains. Therefore, increasing the convective heat transfer coefficient after a ceiling value does not change the order of the total heat transfer rate when the thermal resistance of the convective domain is so small in comparison with the thermal resistance of the conductive domain. In addition, new technologies require significant heat production per unit volume in solid domains, Fig. 1. Carrying this generated heat from solid to cooling channels with less resistance can be achieved with embedding high-conductivity material in the solid domain. However, Ref. [12] shows that high-conductivity material should have a tree-shaped design instead of uniform distribution throughout the solid domain in order to minimize thermal resistance with fixed amount of high-conductivity material.

This paper focuses on cooling performance enhancement with inverted fins which are high-conductivity trees embedded in a non-uniformly heated domain. Because the thermal conductivity of the solid domain is increased with inverted fins, the peak temperature can be kept under an allowable limit with less coolant volume. Therefore, addition of inverted fins in designs which are cooled by convection promise compactness. The literature includes some examples of cooling with embedding high conductivity materials [2, 12-17]. This paper uncovers that the fins should be placed where it is required (where the thermal resistances are significantly greater than others), even it means placing the fins in the solid material.

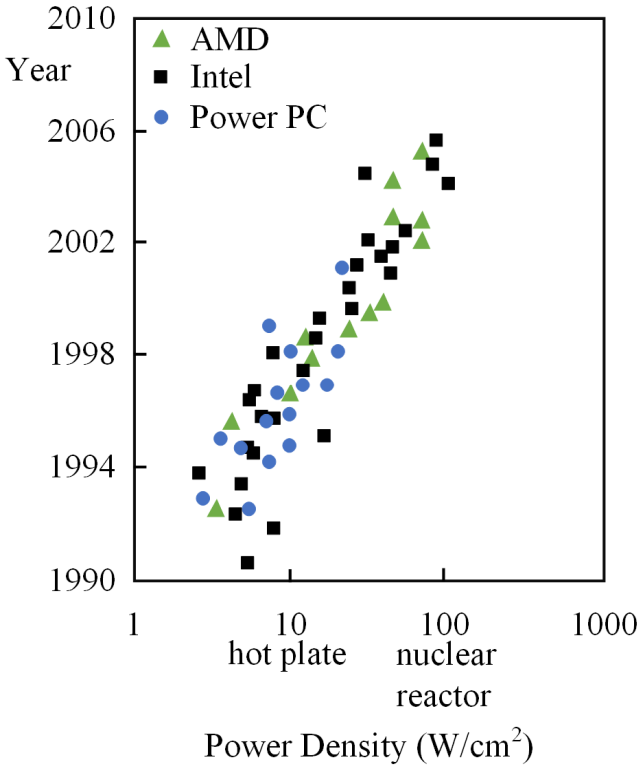

FIGURE 1: TRENDS OF ON CHIP POWER DENSITY BETWEEN THE YEARS 1990 AND 2006, REF [1].

MODEL

Consider a cube which is heated volumetrically with length scale of L, Fig. 2. A cube shaped hot region with length scale of 0.1 L has heat production 100 times greater than the other sections of the solid domain. The heat conductivity of the solid domain is k_l, and a vascular tree with high-conductivity material, k_h, is embedded in the cube to keep it under an allowable peak temperature. The volume fraction between the high-conductivity tree and the low-conductivity cube is φ. The temperature of the tree root, i.e. the heat sink, is T_{ref}, and the outer surfaces of the cube is symmetry boundary condition, $\partial T/\partial n = 0$. The symmetry boundary condition is selected because a number of these elemental cubes will be stacked in palpable devices. Similarly, symmetry boundary condition is used for outer surfaces of heat generating volumes in which high-conductivity material is embedded in the current literature [12-16].

Figure 2 shows the tree design with 2 bifurcation levels (on the left) and the locations of the hot spots (on the right). The governing equations for the low conductivity and high conductivity domains are,

$$k_l \nabla^2 T = q''' \qquad k_l \nabla^2 T = 100 q''' \tag{1}$$

$$k_h \nabla^2 T = 0 \tag{2}$$

where q''' is the volumetric heat rate and $\nabla^2 = \partial^2/\partial x^2 + \partial^2/\partial y^2 + \partial^2/\partial z^2$. The continuity of the heat flux is

$$k_l \frac{\partial T}{\partial n} = k_h \frac{\partial T}{\partial n} \tag{3}$$

The length scale of the nondimensionalization is L.

$$(\tilde{x}, \tilde{y}, \tilde{z}, \tilde{n}) = \frac{(x, y, z, n)}{L} \tag{4}$$

The dimensionless temperature and continuity of heat flux are

$$\tilde{T} = \frac{(T - T_{ref})k_h}{q''' L^2} \tag{5}$$

$$\tilde{k} \left.\frac{\partial \tilde{T}}{\partial \tilde{n}}\right|_h = \left.\frac{\partial \tilde{T}}{\partial \tilde{n}}\right|_l \tag{6}$$

where $\tilde{k} = k_h/k_l$. Heat continuity at the interface of hot region and the rest of the domain reduces to $\partial\tilde{T}/\partial\tilde{n}\big|_{hot} = \partial\tilde{T}/\partial\tilde{n}\big|_{cube}$, i.e. $\tilde{k} = 1$.

The dimensionless governing equations of Eqs. (1) and (2) are

$$\frac{1}{\tilde{k}} \nabla^2 \tilde{T} = 1 \qquad \frac{1}{\tilde{k}} \nabla^2 \tilde{T} = 100 \tag{7}$$

$$\nabla^2 \tilde{T} = 0 \tag{8}$$

NUMERICAL MODEL

Consider the cube with embedded T-shaped tree of Fig. 2. The cube is heated by two heat sources. A cube shaped hot region with length scale of 0.1L which produces $100\,q'''$ and the rest of the domain produces q'''. The vascular tree of Fig. 2 has 2 levels of bifurcation. When the bifurcation level is 0, $L_1 = L$. If the bifurcation level is greater than 0, $L_1 = L/2$ and $L_2 = L_3 = L_4 = L_5 = L_6 = L_7 = L/4$. This length scales are addressed because Ref. [2] shows that there is a length scale corresponding to the smallest heat transfer resistance in high-conductivity tree-shaped inserts. The dimensionless

conductivity is $\tilde{k} = 100$, which corresponds to silicone dioxide and silicone. The reference temperature is $\tilde{T}_{ref} = 0$.

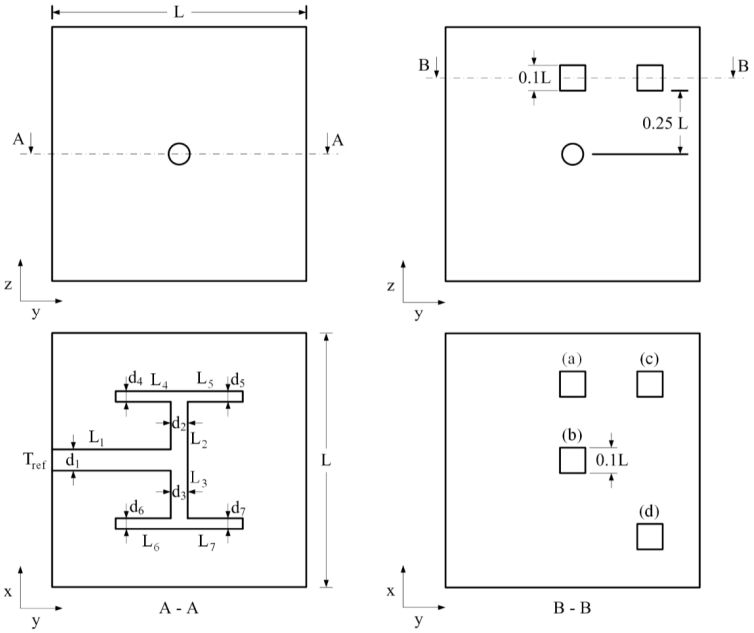

FIGURE 2: HIGH-CONDUCTIVITY TREE EMBEDDED IN A CUBE (LEFT) AND THE LOCATIONS OF THE HOT SPOT (RIGHT).

The dimensionless energy equation was solved by using a finite element software [18]. The grid was non-uniform both in $\tilde{x}$ and $\tilde{y}$ directions, Fig. 3. Figure 3 shows the computation grid for mid-planes of the cube in the x-y (left) and z-x (right) directions. Boundary meshes are used at the interfaces in order to minimize the numerical errors due to variation in the temperature gradients. The mesh size was determined by successive mesh refinement, increasing the number of the mesh elements until the criterion $\left|\left(\tilde{T}^{n}_{max} - \tilde{T}^{n+1}_{max}\right)/\tilde{T}^{n}_{max}\right| < 5\times10^{-3}$ was satisfied. $\tilde{T}^{n}_{max}$ and $\tilde{T}^{n+1}_{max}$ represents the maximum dimensionless temperature by using the current mesh and the refined mesh, respectively. Table 1 illustrates that mesh independency was achieved with 54584 number of mesh when the vascular tree of Fig. 2 has one level of bifurcation with $d_2/d_1 = 0.5$, $d_3/d_1 = 0.5$, $\varphi = 0.01$ and the hot spot is located on (b) of Fig. 2.

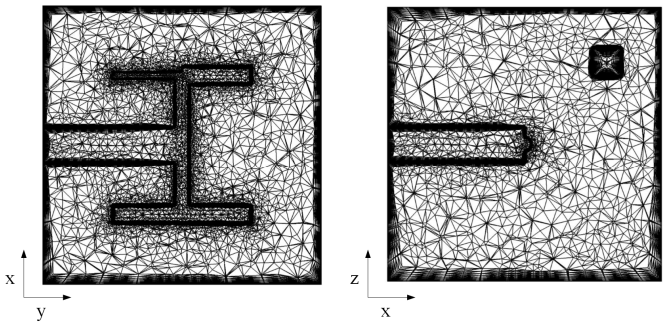

FIGURE 3: COMPUTATION GRID FOR MID-PLANES İN THE X-Y (LEFT) AND Z-X (RIGHT) DIRECTIONS.

The numerical results obtained by using the current method have been compared with the numerical results obtained by Almogbel and Bejan [19] to check the accuracy. The dimensionless governing equations of Ref. [19] was solved with the given geometry and boundary conditions when $\varphi = 0.1$, $H/L = 1$ and $D/B = 0.15$. Table 2 shows that the results of the current numerical method agrees with the results of Ref. [19].

TABLE 1: NUMERICAL TESTS SHOWING THAT MAXIMUM TEMPERATURE DOES NOT DEPEND ON THE MESH SIZE.

Number of elements	$\tilde{T}^{n}_{max}$	$\left\|\left(\tilde{T}^{n}_{max} - \tilde{T}^{n+1}_{max}\right)/\tilde{T}^{n}_{max}\right\|$
12269	0.77994	9.026×10^{-3}
29390	0.78698	1.69×10^{-3}
54584	0.78831	0.279×10^{-3}
127403	0.78809	

In addition, the overall heat transfer rate on the stem surface of the high-conductivity tree is calculated from the numerical simulation as $\tilde{q} = 1.07432$. Because of the outer surfaces of the cube are symmetry boundary condition, the generated heat in the cube should be transferred to the heat sink from the first law of thermodynamics. The rate of the generated heat in the cube is $\tilde{q} = 1.089$, and the error in between the generated heat and the transferred heat was found as 1.3%. This shows that the conservation of the energy was achieved in the numerical solutions.

TABLE 2: COMPARISON OF THE RESULTS OF THE CURRENT STUDY+ AND REF. [19]*.

$\tilde{k}$	$\tilde{T}_{max}$ (FE*)	$\tilde{T}_{max}$ (FD*)	$\tilde{T}_{max}$ (Comsol+)
1000	0.128236	0.128979	0.12847
300	0.135924	0.135408	0.13616
100	0.157219	0.152994	0.15745
30	0.224812	0.218397	0.22509
10	0.374893	0.37539	0.37559

HIGH-CONDUCTIVITY TREES

Figure 4 shows the temperature distribution in the cube with the vascular tree of N = 2 for the hot spot locations of Fig. 2. Red and blue represent the maximum and the minimum temperatures. The peak temperatures of the each cube are: a) $\tilde{T}_{max} = 0.72$, b) $\tilde{T}_{max} = 0.62$, c) $\tilde{T}_{max} = 0.74$ and d) $\tilde{T}_{max} = 0.63$. The temperature distribution of Figs. 4b and 4d is more uniform than Figs. 4a and 4c.

Figure 5 shows the evolution of $\tilde{T}_{max}$ and $\tilde{T}_{avg}$ relative to φ when N = 0. $\tilde{T}_{max}$ and $\tilde{T}_{avg}$ decrease as φ increases. In addition, the decrease in the maximum temperature diminishes as φ increases. This result is expected because increasing the amount of the high-conductivity material both decreases the overall heat transfer resistance and the overall heat generation rate. The overall heat generation rate decreases because the high-conductivity insert have zero heat generation.

Next consider the tree design with one level of bifurcation, i.e. the branches of diameter d_1, d_2 and d_3 exist in Fig. 2. The location of the hot spot is as shown in Fig. 2 (a). For $\varphi = 0.01$, the diameter ratios of d_2/d_1 and d_3/d_1 are varied respectively to find the tree design which provides the smallest peak temperature, Fig. 6. First, d_3/d_1 was fixed at 0.5 and d_2/d_1 was varied, and the peak temperature is smallest with $d_2/d_1 = 0.4$. Then, the optimized value of $d_2/d_1 = 0.4$ was fixed, and d_3/d_1 was varied. The peak temperature is the smallest when $d_2/d_1 = 0.4$ and $d_3/d_1 = 0.4$, Fig. 6.

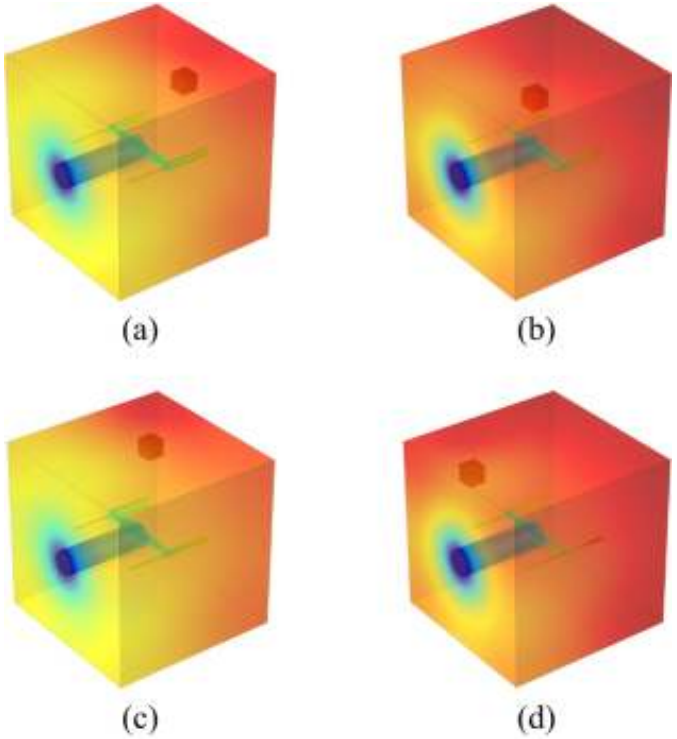

FIGURE 4: TEMPERATURE DISTRIBUTION IN THE CUBE WITH AN INSERTED HOT SPOT, RED AND BLUE REPRESENT MAXIMUM AND MINIMUM TEMPERATURES, RESPECTIVELY.

Figure 7 (top) shows the evolution of $\tilde{T}_{max}$ and $\tilde{T}_{avg}$ when φ varies with one level of bifurcation. The optimal diameter ratios of Fig. 6 ($d_2/d_1 = 0.4$ and $d_3/d_1 = 0.4$) are used as the diameter ratios. $\tilde{T}_{max}$ and $\tilde{T}_{avg}$ decrease as φ increases. Figure 7 (bottom) compares the peak temperatures of the Figs. 5 and 7 (top). Figure 7 (bottom) shows that when the volume fraction is 0.005, using the design with one level of bifurcation provides the smallest peak temperature. When φ = 0.015, the peak temperature of N = 0 and N = 1 designs become the same. This volume fraction value is the transition point of design. The design should be changed from N = 1 to N = 0 in order to minimize peak temperature as φ increases. This shows that as the size of the system changes, the shape of the high-conductivity insert should also change. This result is in accord with the constructal theory, and Ref. [20] also shows how the miniature of a system should have a different shape in order to minimize resistances.

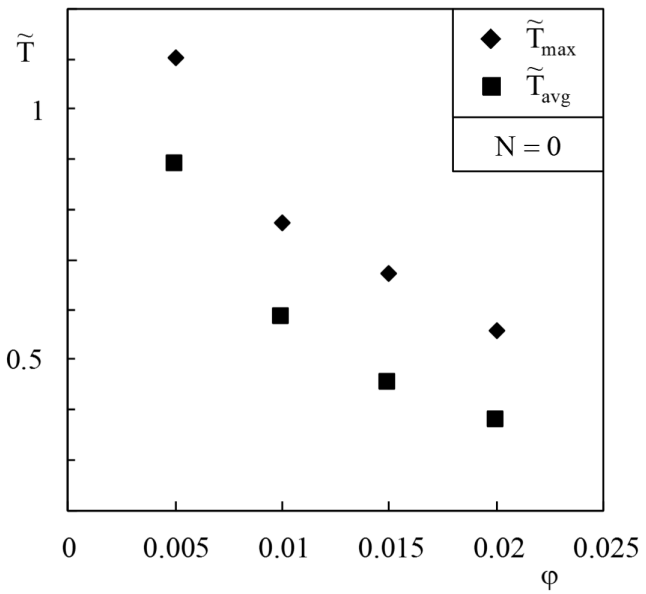

FIGURE 5: THE EFFECT OF φ ON THE PEAK AND AVERAGE TEMPERATURES WITH N = 0.

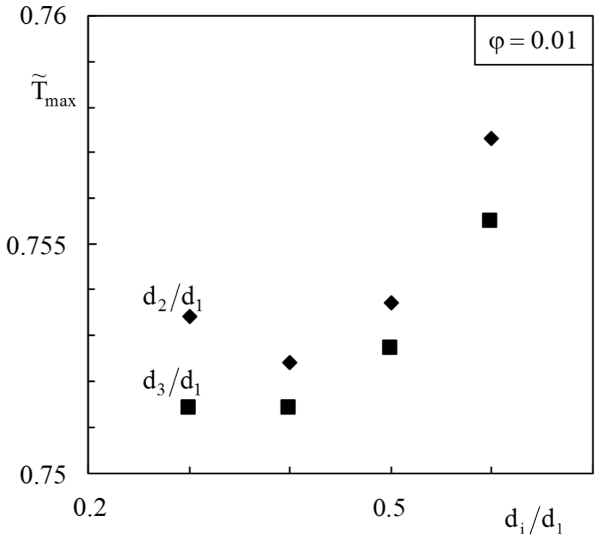

FIGURE 6: THE EFFECT OF d_2/d_1 AND d_3/d_1 RATIOS ON THE PEAK TEMPERATURE WHEN N = 1 AND φ = 0.01.

Figure 8 documents the minimum peak temperatures and corresponding diameter ratios relative to the hot spot locations. For each hot spot location, only the minimum peak temperatures are documented, i.e. the optimal values are found with repeating the procedure of creating Fig. 6. Figure 8 (top) shows how $\tilde{T}_{max}$ and $\tilde{T}_{avg}$ are affected from the location of the hot spot. $\tilde{T}_{max}$ is smaller when the hot spot is located in (b) or (d) of the Fig. 2, i.e. when the hot spot is closer to the trunk of the vascular tree. In addition, $\tilde{T}_{avg}$ was not affected much from the location of the hot spot. However, the temperature distribution in the cube is more uniform (the order of $\tilde{T}_{max}$ and $\tilde{T}_{avg}$ closer to each other) in the hot spot locations (b) and (d) than in the hot spot locations (a) and (c) of Fig. 2, Fig. 8. Figure 8 (bottom) shows how the diameter ratios of d_2/d_1 and d_3/d_1 (which correspond to the smallest peak temperature) vary relative to the location of the hot spot. The ratios of d_2/d_1 and d_3/d_1 should be the same when the hot spot is located at (a) in Fig. 2 as shown in Fig. 8. The reason of this is that the hot spot has the same distance to the branches of d_2 and d_3, and it is in the symmetry plane of the vascular tree.

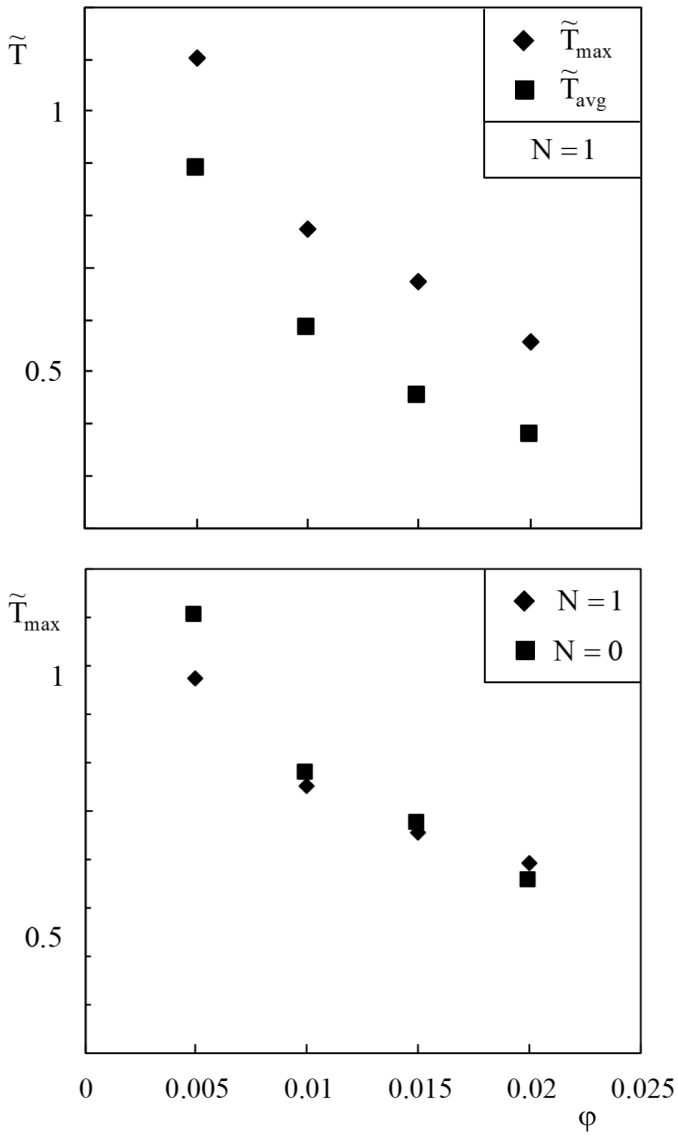

FIGURE 7: THE EFFECT OF φ ON: $\tilde{T}_{max}$ AND $\tilde{T}_{avg}$ WHEN N = 1 (TOP) AND $\tilde{T}_{max}$ WHEN N = 0 AND 1 (BOTTOM).

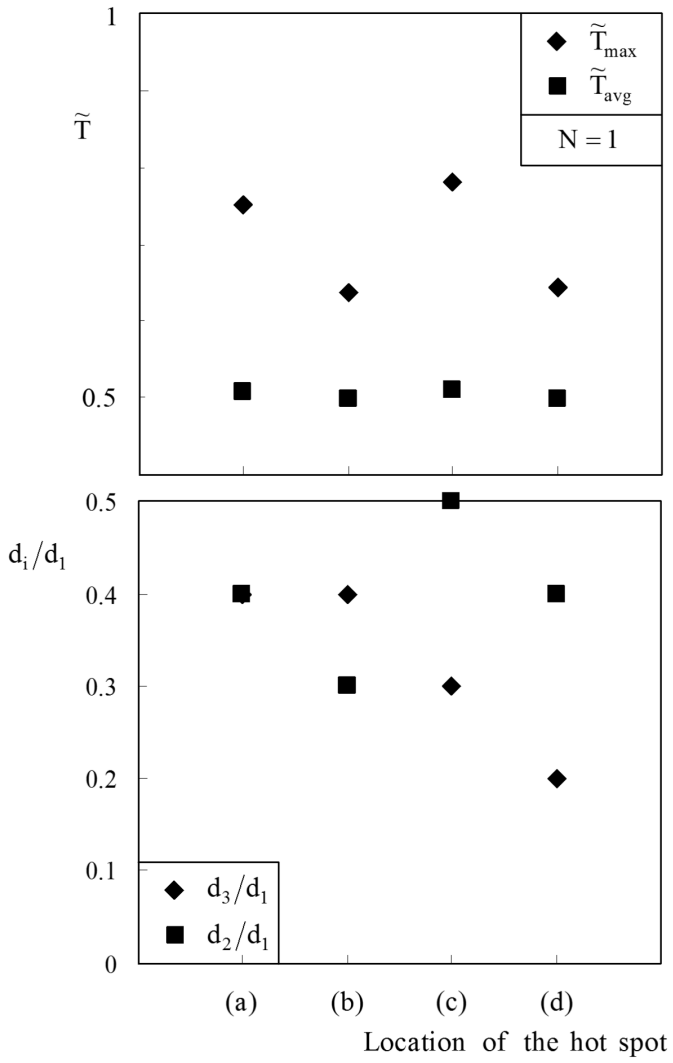

FIGURE 8: THE EFFECT OF THE HOT SPOT LOCATION ON $\widetilde{T}_{max}$ AND $\widetilde{T}_{avg}$ WHEN φ = 0.01 AND N = 1 (TOP). OPTIMIZED DIAMETER RATIOS OF d_2/d_1 AND d_3/d_1 RELATIVE TO THE HOT SPOT LOCATIONS (BOTTOM).

Figure 9 (top) shows how $\widetilde{T}_{max}$ and $\widetilde{T}_{avg}$ are affected by the location of the hot spot when high-conductivity tree has two levels of bifurcation. The minimum peak temperatures shown in Fig. 9 are smaller than in Fig. 8, i.e. peak temperature is decreased by adding the second levels of bifurcation when $\varphi = 0.01$. Figure 9 (bottom) shows the diameter ratios corresponding to the minimum peak temperature for each location of the hot spot. The diameter ratios of d_2/d_1 and d_3/d_1 are the ratios correspond to the minimum peak temperature in Fig. 8 (bottom). The peak temperature decreases as the diameter ratios of d_4/d_1 and d_6/d_1 decrease. However, the diameter ratios of d_4/d_1 and d_6/d_1 have been decreased to a ratio such that the mesh does not affect the results by more than 0.5%, and this ratio is $d_4/d_1 = d_6/d_1 = 0.05$.

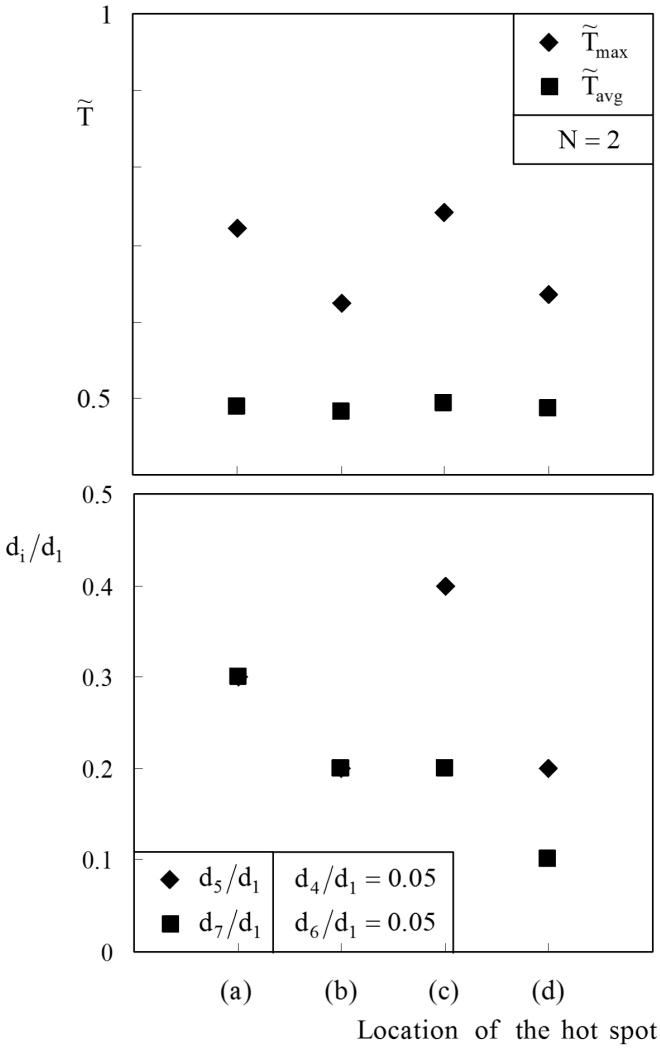

FIGURE 9: THE EFFECT OF THE HOT SPOT LOCATION ON $\widetilde{T}_{max}$ AND $\widetilde{T}_{avg}$ WHEN φ = 0.01 AND N = 2 (TOP). OPTIMIZED DIAMETER RATIOS OF THE TREE DESIGN RELATIVE TO THE HOT SPOT LOCATIONS (BOTTOM).

Figure 10 shows how $\widetilde{T}_{max}$ changes relative to the hot spot location as the number of the bifurcation level increases. Tree designs of N = 1 and N = 2 are the designs correspond to the minimum peak temperature of Fig. 8 and Fig. 9, respectively. N = 2 design provides the smallest and N = 0 design provides the greatest $\widetilde{T}_{max}$ for the given design parameters and boundary conditions. Depending on the hot spot location, the transition point from N = 1 to N = 2 design changes. For example, when the hot spot is located at (d) in Fig. 2, the design of N = 1 provides the same cooling performance as the design of N = 2.

When the hot spot location is (c), changing from N = 1 to N = 2 decreases $\widetilde{T}_{max}$.

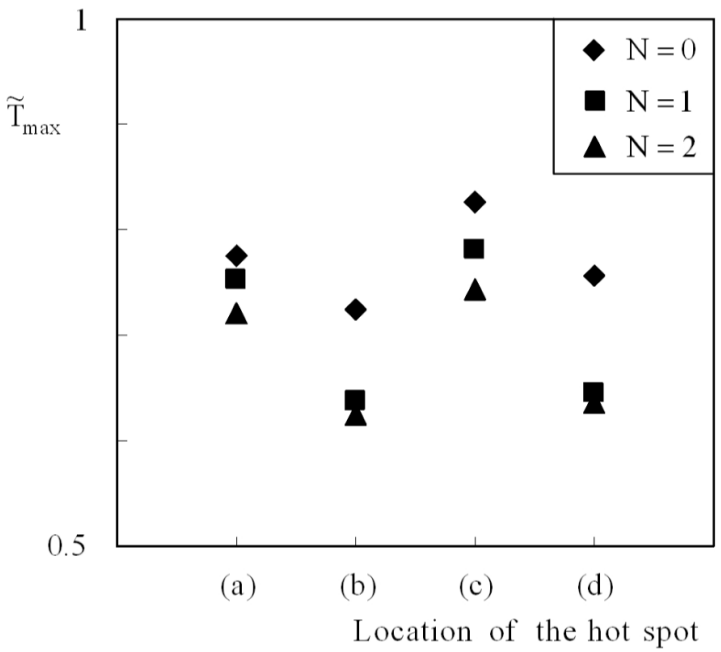

FIGURE 10: THE EFFECT OF THE HOT SPOT LOCATION ON $\widetilde{T}_{max}$ FOR THE DESIGNS OF N = 0, 1 AND 2 WHEN φ = 0.01.

Y-SHAPED TREES

Figure 9 (bottom) shows that the peak temperature is the smallest when d_4/d_1 and d_6/d_1 diameter ratios reaches to 0. This result suggests that removing the branches of diameter d_4 and d_6 could decrease the conductive thermal resistance because the amount of high-conductivity material is fixed. The literature also shows that Y-shaped trees provide greater cooling performance than T-shaped trees [12, 21-22].

Figure 11 shows the evolution of $\widetilde{T}_{max}$ when the bifurcation angle varies. The diameter ratios of d_2/d_1 and d_3/d_1 are the optimized ratios shown in Fig. 8 (bottom). T-shaped tree design of Fig. 8 (top) has $\theta = 180^\circ$. Decreasing θ from 180 to 60 decreases $\widetilde{T}_{max}$, and if θ continues to be decreased then $\widetilde{T}_{max}$ increases. $\theta = 60^\circ$ provides the minimum peak temperature when the hot spot is located at (a) in Fig. 2. Y-shaped trees promise lower conductive thermal resistance than T-shaped trees with the same amount of high-conductivity material.

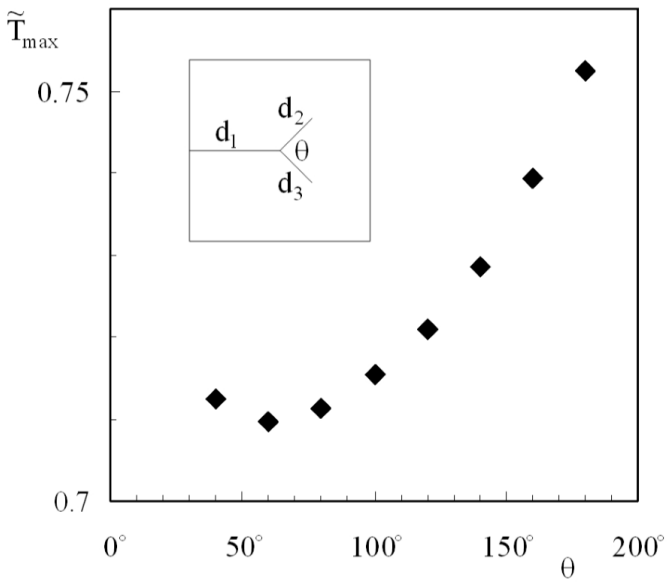

FIGURE 11: THE EVOLUTION OF $\widetilde{T}_{max}$ RELATIVE TO THE BIFURCATION ANGLE WHEN φ = 0.01.

The hot spot creates non-uniform heating throughout the cube. Therefore, the location of the vascular tree in the z direction also affects the cooling performance of the vascular tree. Locating the vascular tree such that it touches to the hot spot decreases the heat transfer resistance because the distance (and conductive thermal resistance) in between the hot spot and the vascular tree decreases. However, the heat transfer resistance from the remaining sections of the cube increases when the vascular tree touches to the hot spot because the distance between the lower edge of the cube and the vascular tree increases. There is a trade off in between these two thermal resistances. Therefore, there should be a location for the vascular tree that provides the minimum peak temperature which is closer to the hot spot but not touches it.

Figure 12 shows the evolution of $\widetilde{T}_{max}$ relative to the location of the vascular tree in the z direction when N = 1 for T- and Y-shaped tree designs. $\widetilde{T}_{max}$ decreases as the location of the vascular tree changes from z = 0.5 L to z = 0.65 L. Placing the stem of the high-conductivity tree at z = 0.65L minimizes total conductive heat transfer resistance from the entire cube to the vascular tree when the hot spot is located on (a) of Fig. 2 and φ = 0.01. Even though hot spot is located on z = 0.75 L, z = 0.65L location provides the smallest peak temperature.

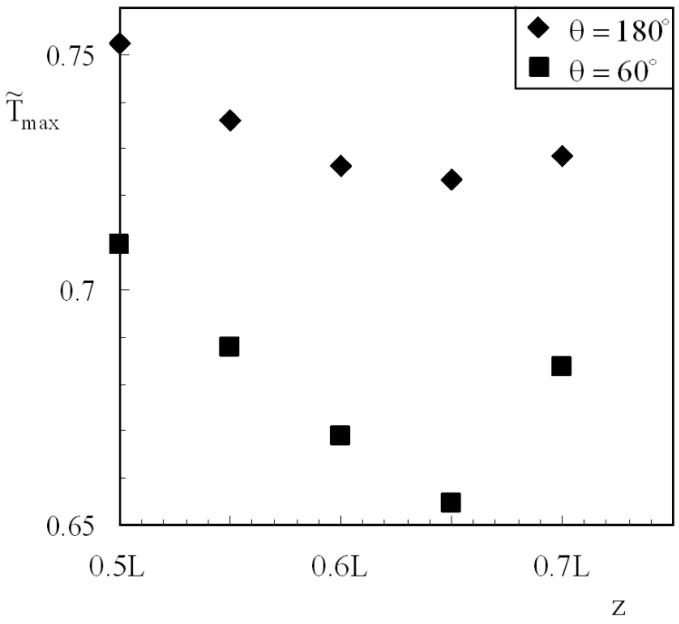

FIGURE 12: THE EVOLUTION OF $\tilde{T}_{max}$ RELATIVE TO THE VASCULAR TREE LOCATION IN THE Z DIRECTION WHEN φ = 0.01.

CONCLUSIONS

This paper shows that inverted fins are capable of decreasing the overall thermal resistance of a non-uniformly heated cube. The cooling system becomes more compact with the inverted fins because the required coolant volume decreases. Increasing the volume fraction of the high-conductivity material decreases the peak temperature when the number of the bifurcation level is fixed. In addition, increasing the number of the bifurcation levels decreases the peak temperature when φ decreases. There is a transition point from one high-conductivity tree design to another for each volume fraction value.

This paper also shows how the diameters of the tree branches should be changed in order to minimize the peak temperature. The diameter ratios corresponding to the smallest peak temperatures are documented for variable hot spot locations. Depending on the location of the hot spot, the merit of increasing the number of the bifurcation levels also changes. In addition, the effects of the bifurcation angle and the location of the vascular tree in the z direction are uncovered. The design with $\theta = 60^\circ$ and stem location of $z = 0.65L$ provides the smallest peak temperature.

In addition, the optimal diameter ratios of Fig. 8 (bottom) and Fig. 9 (bottom) show that tree branches with diameters of d_4 and d_6 are unnecessary. The thermal boundary layer of the stem cools the region where these two branches are located. Because Y-shaped trees do not have the branches with diameters of d_4 and d_6, Y-shaped trees provide smaller peak temperatures than T-shaped trees. The overall conductive thermal resistance can be decreased if the boundary layers of the high-conductivity branches just touch each other to cover the greatest volume. Constructal law states that inserting the material where it is needed decreases the imperfection [2]: the results of this paper agree with that statement, i.e. fins should be placed in the solid material when the thermal resistance of the conductive domain is greater than the thermal resistance of the convective domain.

Producing a structure with embedded inverted fins is a manufacturing challenge. However, with the new production methods such as additive manufacturing it is possible, and a decade or so it may become feasible. In addition, simple structures (such as structures with zero and one level of bifurcation) can be manufactured. The simple structures would decrease the peak temperature. However, Figure 7 shows that as volume fraction decreases the complexity of the design should increase in order to minimize the peak temperature.

NOMENCLATURE

B length of k_p blade, m, Ref. [19]
D thickness of k_p blade, m, Ref. [19]
d diameter of high-conductivity tree branch, m, Fig. 1
H height of conducting domain, m, Ref. [19]
k thermal conductivity, W m^{-1} K^{-1}
L length scale of the cube (Fig. 2) and length of conducting domain of Ref. [19], m
n normal direction
N number of bifurcation levels
$\tilde{q}$ dimensionless overall heat transfer rate
q''' heat source, W m^{-3}
T temperature, K
x, y, z coordinates, m

Greek symbols

φ volume fraction
θ bifurcation angle

Subscripts

avg average
cube cube of length scale L
h high
hot hot spot of length scale 0.1L
l low
max maximum
ref reference

Superscript

n index of the mesh independency test
~ dimensionless

ACKNOWLEDGMENTS

This work was supported by the Republic of Turkey. Almogbel and Bejan's [19] data was used in this paper for the validation process. The author wishes to thank him for his contribution to the subject of conductive cooling.

REFERENCES

[1] Pop E, Sinha S, Goodson KE. Heat generation and transport in nanometer-scale transistors. *Proceedings of the IEEE* 2006; **94**, pp. 1587−1601, DOI: 10.1109/JPROC.2006.879794.

[2] Bejan A, Lorente S. *Design with Constructal Theory* 2008, Wiley, Hoboken.

[3] Said, SAM. Investigation of natural convection in convergent vertical channels. Int. J. Energy Res. 1996; 20, pp. 559−567, DOI: 10.1002/(SICI)1099-114X(199607)20:7<559::AID-ER115>3.0.CO;2-J.

[4] Jang D, Yook S-J, Lee K-S. Optimum design of a radial heat sink with a fin-height profile for high-power led lighting applications. Appl. Energy 2014; 116, pp. 260−268, DOI: 10.1016/j.apenergy.2013.11.063.

[5] Kim YS, Lorente S, Bejan A. Constructal steam generator architecture. Int. J. Heat Mass Transfer 2009; 52, pp. 2362−2369, DOI: 10.1016/j.ijheatmasstransfer.2008.10.021.

[6] Bejan A, Lorente S. Constructal multi-scale and multi-objective structures. *Int. J. Energy Res.* 2005; **29**, pp. 689−710, DOI: 10.1002/er.1100.

[7] Ho T, Mao SS, Greif R. Improving efficiency of high-concentrator photovoltaics by cooling with two-phase forced convection. *Int. J. Energy Res.* 2010; **34**, pp. 1257−1271, DOI: 10.1002/er.1670.

[8] Cetkin E, Lorente S, Bejan A. Hybrid grid and tree structures for cooling and mechanical strength. *J. Appl. Phys.* 2011; **110** 064910, DOI: 10.1063/1.3626062.

[9] Lorente S, Bejan A, Niu JL. Phase change heat storage in an enclosure with vertical pipe in the center. *Int. J. Heat Mass Transfer* 2014; **72**, pp. 329−335, DOI: 10.1016/j.ijheatmasstransfer.2014.01.021.

[10] Kakac S, Pramuanjaroenkij A. Review of convective heat transfer enhancement with nanofluids. *Int. J. Heat Mass Transfer* 2009; **52**, pp. 3187−3196, DOI: 10.1016/j.ijheatmasstransfer.2009.02.006.

[11] Eastman JA, Choi SUS, Li S, Yu W, Thompson LJ. Anomalously increased effective thermal conductivities of ethylene glycol-based nanofluids containing copper nanoparticles. *Appl. Phys. Lett.* 2001; **78**, pp. 718−720, DOI: 10.1063/1.1341218.

[12] Cetkin E. Three-dimensional high conductivity trees for volumetric cooling. *Int. J. Energy Res.* 2014; published online, DOI: 10.1002/er.3176.

[13] Bejan A. Constructal tree-shaped paths for conduction and convection. *Int. J. Energy Res.* 2003; **27**, pp. 283−299, DOI: 10.1002/er.875.

[14] Bejan A. Constructal-theory network of conducting paths for cooling a heat generating volume. *Int. J. Heat Mass Transfer* 1997; **40**, pp. 799–816, DOI: 10.1016/0017-9310(96)00175-5.

[15] Rocha LAO, Lorente S, Bejan A. Conduction tree networks with loops for cooling a heat generating volume. *Int. J. Heat Mass Transfer* 2006; **49**, pp. 2626−2635, DOI: 10.1016/j.ijheatmasstransfer.2006.01.017.

[16] Ledezma GA, Bejan A, Errera MR. Constructal tree Networks for heat transfer. *J. Appl. Phys.* 1997; **82**, pp. 89−100, DOI: 10.1063/1.365853.

[17] Ledezma GA, Bejan A. Constructal three-dimensional trees for conduction between a volume and one point. *J. Heat Transfer* 1998; **120**, pp. 977−984, DOI: 10.1115/1.2825918.

[18] See www.comsol.com for information about Comsol Multiphysics.

[19] Almogbel M, Bejan A. Conduction trees with spacings at the tips. *Int. J. Heat Mass Transfer* 1999; **42**, pp. 3739−3756, DOI: 10.1016/S0017-9310(99)00051-4.

[20] Cetkin E, Lorente S, Bejan A. Natural constructal emergence of vascular design with turbulent flow. *J. Appl. Phys.* 2010; **107** 114901, DOI: 10.1063/1.3430941.

[21] Cetkin E, Lorente S, Bejan A. The steepest S curve of spreading and collecting flows: Discovering the invading tree, not assuming it. *J. Appl. Phys.* 2012; **111** 114903, DOI: 10.1063/1.4721657.

[22] Kobayashi H, Lorente S, Anderson R, Bejan A. Freely morphing tree structures in a conducting body. *Int. J. Heat Mass Transfer* 2012; 55, pp. 4744−4753, DOI: 10.1016/j.ijheatmasstransfer.2012.04.038.